Structure of endohedral fullerene Eu@C_{74}†

Dmitrij Rappoport* and Filipp Furche

Received 2nd February 2009, Accepted 12th May 2009
First published as an Advance Article on the web 10th June 2009
DOI: 10.1039/b902098e

Structure determination of endohedral fullerenes in the absence of X-ray data is difficult and often controversial. Here we show that the structure of endohedral fullerene Eu@C_{74} may be determined by density functional theory aided interpretation of its electronic, infrared and Raman spectra. The use of recently developed analytical polarizability gradient methods to simulate resonance-enhanced Raman spectra is crucial for this approach and allows for a nearly complete assignment of the experimental spectra. Eu@C_{74} is assigned a pear-shaped C_{2v} symmetric structure and shows strong ionic interaction between the encapsulated metal and the fullerene π system.

1. Introduction

Endohedral metallofullerenes constitute a large class of fullerene inner complexes with metal atoms or small metal clusters.[1,2] Group 2 and 3 metals and lanthanides form a number of endohedral fullerene complexes notable for their electronic absorption in the near infrared and for their large third-order nonlinear susceptibilities.[1–3] Lanthanide endohedral fullerenes have recently attracted attention as high-relaxivity contrast agents for magnetic resonance imaging[4,5] and as spin qubits for quantum computing.[6]

A major challenge in endohedral fullerene chemistry is the complicated preparation and purification procedure yielding only milligrams or less of substance.[1,7] Structure determination by X-ray crystallography is further complicated by the low crystallization tendency of fullerenes and crystal disorder.[8] These difficulties may be alleviated by co-crystallization with metalloporphyrins, *e.g.*, for $Tb_3N@C_{80}$[9] or $Ba@C_{74}$[10] or using covalent adducts such as $La@C_{74}C_6H_3Cl_3$.[11] Nevertheless, experimental structural data are still unavailable for many fullerene metal complexes including all europium endohedral fullerenes. Eu@C_{74} was the first isolated endohedral europium fullerene and was characterized spectroscopically and electrochemically ten years ago.[12] However, the structure of Eu@C_{74} has not been established to date.

In a pioneering study, Vietze, Seifert and Fowler (VSF) applied semi-empirical density functional tight-binding theory (DFTB) methods to Eu@C_{74}.[13] Their work focused on tentative structures and relative energies of low-lying isomers. VSF did not provide predictions of experimentally accessible properties of Eu@C_{74}, and thus a conclusive assignment of the structure was not possible. Here we show how modern density functional methods can help to extract structural information from electronic, infrared and Raman spectra of Eu@C_{74}. This leads to the first definitive structure assignment of this endohedral fullerene. We compare the electronic excitation spectrum of Eu@C_{74} to predictions from time-dependent density functional theory (TDDFT) to identify the frontier molecular orbitals, specifically the electronic configuration of europium. The structure of the carbon cage is inferred from an assignment of infrared and Raman spectra of Eu@C_{74}.

An important tool in the structure elucidation of endohedral fullerenes is ^{13}C nuclear magnetic resonance (NMR) spectroscopy. ^{13}C NMR was used in conjunction with density functional calculations to determine the structures of the closed-shell endohedral fullerenes Ca@C_{74}[14] and Yb@C_{74}.[15] However, no ^{13}C NMR data have been reported for Eu@C_{74} which makes the present theory-aided interpretation of electronic and vibrational spectra particularly useful. The present approach is applicable to other paramagnetic endohedral fullerenes.

2. Computational details

The theoretical tools for prediction of the vibrational properties of Eu@C_{74} are based on analytical derivative methods in the framework of density functional theory (DFT). Molecular force constants of large molecules are efficiently computed from analytical second energy derivatives with respect to nuclear displacements.[16,17] However, due to the large number of vibrations and the low symmetry of Eu@C_{74}, vibrational frequencies alone contain too little information for a complete vibrational band assignment. Infrared intensities and Raman scattering cross sections provide additional characterization and are essential for correlating computed vibrational modes to observed bands in vibrational spectra of Eu@C_{74}.

The present structural assignment of Eu@C_{74} became possible by the recently developed efficient method for computing Raman scattering cross sections in the framework of TDDFT.[18] Within polarizability theory, Raman scattering cross sections are determined from first-order derivatives of the frequency-dependent polarizability with respect to normal-mode displacements.[19,20] Efficient computation of polarizability derivatives has long been the time-limiting step in Raman calculations. Methods based on numerical differentiation of frequency-dependent polarizabilities were

Department of Chemistry, University of California, Irvine, CA 92697-2025, USA. E-mail: d.rappoport@uci.edu
† Electronic supplementary information (ESI) available: Atomic coordinates. See DOI: 10.1039/b902098e

applied to the molecules as large as buckminsterfullerene C_{60},[21] exploiting its high point group symmetry. The major drawback of numerical derivative methods is that they require a large number of polarizability evaluations that increases with the number of nuclear degrees of freedom. In contrast, the recently proposed analytical derivative method based on a Lagrangian formulation of frequency-dependent polarizabilities[18] yields *all* Cartesian polarizability derivatives at approximately 2–3 times the cost of a single polarizability calculation, independent of the number of nuclear degrees of freedom. In contrast to the widely used analytical Hartree–Fock-based implementation of Frisch and co-workers,[22] the Lagrangian method[18] includes the frequency-dependence of polarizability derivatives in a natural way. This is particularly important for molecules with low excitation energies such as fullerenes because resonance enhancement is significant at experimental excitation frequencies.[23,24]

The structures of the energy minima and transition states of Eu@C_{74} were optimized in C_{2v} point group symmetry using the BP86 exchange–correlation functional[25,26] and the resolution of the identity approximation (RI-*J*).[27] Basis sets were of split-valence quality with polarization (SVP) for carbon[28] and of triple-zeta valence quality with two sets of polarization functions (TZVPP) for europium[29] together with corresponding auxiliary basis sets.[27,29] Effective core potentials (ECP) were used for europium.[30] Reoptimization of the energy minimum structure using triple-zeta valence quality basis set on all atoms resulted in changes in bonding distances of 1 pm or less. Thus, SVP basis sets were used for carbon atoms, and TZVPP basis sets were used for europium for all structure optimizations and force constant calculations in this study. Electronic excitation energies and oscillator strengths were obtained from TDDFT calculations[31,32] using the RI-*J* approximation.[33] The exchange–correlation functional and basis sets were the same as above. The electronic excitation spectrum of Eu@C_{74} was simulated by Gaussian broadening of the calculated line spectrum using an empirical linewidth of 0.05 eV.

Vibrational frequencies and infrared intensities were computed from analytical second energy derivatives[16] in the RI-*J* approximation.[17] Raman scattering cross sections were computed from analytical derivatives of frequency-dependent polarizabilities[18] at $\lambda = 514.54$ nm excitation wavelength using the PBE0 hybrid functional.[34] Polarizability derivative calculations employed diffusely augmented SVPs basis sets for carbon;[35] the basis set for europium was constructed by 1s1p1d1f augmentation of the TZVPP basis set. The exponents for the diffuse basis functions were obtained by downward extrapolation. The calculated infrared and Raman line spectra were broadened using Gaussians of 4 cm^{-1} linewidth. Frequency scaling was not applied since the scaling factor for the BP86 functional is almost unity.[36] All calculations were performed using TURBOMOLE program package.[37]

We restricted our analysis to structures derived from the D_{3h} isomer of C_{74} fullerene which satisfies the isolated pentagon rule (IPR). Non-IPR structures were found to be considerably less stable for empty C_{74}[38] as well as for its endohedral complexes.[13,39]

3. Results and discussion

3.1 Minimum energy structure

The empty C_{74} cage is known to have a D_{3h} symmetric structure.[38] In Eu@C_{74} the carbon cage is distorted from D_{3h} symmetry along one of the three equivalent dihedral axes. The resulting three degenerate energy minima have symmetry-equivalent C_{2v} symmetric structures one of which is depicted in Fig. 1. The europium atom is symmetrically coordinated to a [6,6]-bond of a pyracyclene unit with europium–carbon distances of 254 pm. Four carbon atoms adjacent to the coordinated [6,6]-bond are at a distance of 267 pm from europium, which is even shorter than the europium–carbon distances of 277–282 pm found in the europium cyclopentadienyl complex $Eu(C_5Me_5)_2$.[40–42] The carbon cage is visibly distorted near the encapsulated metal: the cage surface is bulged out at the coordination site while the coordinated C–C bond is elongated by 6 pm compared to the empty C_{74} cage.

The formation of the Eu@C_{74} endohedral complex from neutral species is associated with a large binding energy of 359 kJ mol^{-1}. The counterpoise correction for the basis set superposition error (BSSE) reduces the binding energy to 324 kJ mol^{-1}. The three energy minima of Eu@C_{74} are symmetry-equivalent, in agreement with only one Eu@C_{74} fraction found in the HPLC separation procedure.[12] The degenerate interconversion of neighboring energy minima proceeds *via* a C_{2v}-symmetric transition state with a sizeable activation barrier of 46 kJ mol^{-1} (42 kJ mol^{-1} including the BSSE correction). As a consequence, the diffusional motion of the europium atom throughout the carbon cage is strongly hindered. ^{13}C-NMR experiments on Ca@C_{74} showed that the site-hopping motion of the calcium atom is observable at the time scale of the NMR experiment.[14] An activation barrier of 29–38 kJ mol^{-1} was computed for interconversion in Ca@C_{74} using the B3LYP functional and small basis sets.[39] Using the same level of theory as for Eu@C_{74} (BP86 functional, SVP basis set for carbon, TZVPP basis set for calcium) we obtained an even larger barrier of 47 kJ mol^{-1} (not including the BSSE correction). The characteristic time scale of NMR experiments is several orders of magnitude slower than that of vibrational

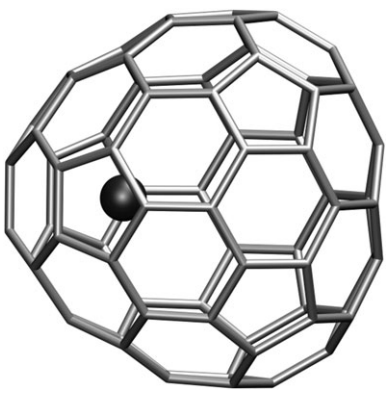

Fig. 1 The computed minimum structure of fullerene Eu@C_{74}. Two further symmetry-equivalent structures are obtained by rotating the position of the Eu atom about the C_3 axis of the empty cage.

and electronic spectroscopy. Thus the findings for $Ca@C_{74}$ corroborate our assumption that the present static picture of $Eu@C_{74}$ disregarding large-amplitude motions of europium is adequate for the interpretation of its electronic and vibrational spectra.

3.2 Electronic excitation spectrum

The electronic excitation spectrum of $Eu@C_{74}$ (Fig. 2) features absorption bands in the visible and near infrared region below 2000 nm. The experimental spectrum in carbon disulfide from ref. 12 is shown in Fig. 2 along with TDDFT results. The computed electronic excitation energies and oscillator strengths for the stronger electronic excitations are given in Table 1 along with a tentative assignment of the experimental spectrum. The lowest excitation (B_1 symmetry) is calculated at 0.45 eV (2780 nm); due to its low oscillator strength it is absent in the experimental spectrum. The position of the first observable absorption band (band A) at 0.63 eV (1969 nm) compares well with the predicted excitation energy of 0.59 eV (2113 nm). Both excitation bands arise from $\pi \rightarrow \pi^*$ transitions in the fullerene cage. The experimental bands B and C at 0.80 eV (1549 nm) and 1.04 eV (1192 nm), respectively, are composed of several closely lying $\pi \rightarrow \pi^*$ and charge-transfer transitions from Eu 4f orbitals into the π system of the fullerene.

3.3 Vibrational spectra

The calculated and experimental infrared spectra of $Eu@C_{74}$ are displayed in Fig. 3. The computed Raman spectrum of $Eu@C_{74}$ is compared to the experimental spectrum at 514.5 nm excitation wavelength in Fig. 4. Experimental infrared and Raman spectra of solid $Eu@C_{74}$ are taken from ref. 12. Previous studies have shown that Raman scattering cross sections are consistently overestimated by 10–15% with the PBE0 functional.[18] In addition, environment effects in the solid phase of $Eu@C_{74}$ as well as limited experimental resolution render a detailed comparison between theoretical predictions and the experimental spectrum currently impossible. Thus, we limit ourselves to the assignment of strong vibrational bands and the comparison of the spectral shapes between theory and experiment. The resulting assignment is shown in Table 2. In total, 38 vibrational bands in the infrared and Raman spectra of $Eu@C_{74}$ were assigned to fundamental transitions. Almost all intense bands found in the experiment could be identified with intense vibrational transitions in the computed spectra, and *vice versa*. Within our assignment, the mean absolute

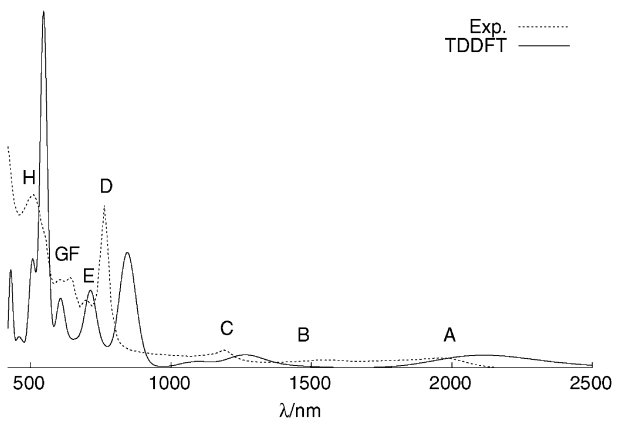

Fig. 2 Experimental and calculated electronic excitation spectrum of $Eu@C_{74}$. Experimental data are from ref. 12.

Table 1 Computed near-infrared electronic excitation energies and oscillator strengths (in dipole-length gauge) of $Eu@C_{74}$. Symmetry labeling according to irreducible representations of C_{2v} point group. Band labels from Fig. 2

Exp.[12]		TDDFT			
Band	λ/nm	Exc.	λ/nm	$f \times 10^3$	Characterization
A	1969	$2\ ^8B_1$	2113	2.5	$\pi \rightarrow \pi^*$
B	1549	$2\ ^8A_1$	1485	0.1	$\pi \rightarrow \pi^*$
		$1\ ^8B_2$	1424	2.8	Eu(4f) $\rightarrow \pi^*$
C	1192	$3\ ^8A_1$	1273	1.0	Eu(4f) $\rightarrow \pi^*$
		$4\ ^8A_1$	1262	2.4	$\pi \rightarrow \pi^*$, Eu(4f) $\rightarrow \pi^*$
D	763	$8\ ^8A_1$	846	20.9	$\pi \rightarrow \pi^*$, Eu(4f) $\rightarrow \pi^*$
		$7\ ^8B_1$	828	2.1	Eu(4f) $\rightarrow \pi^*$
E	697	$10\ ^8A_1$	718	5.5	$\pi \rightarrow \pi^*$
		$11\ ^8B_1$	709	6.2	$\pi \rightarrow \pi^*$, Eu(4f) $\rightarrow \pi^*$
F	643	$13\ ^8B_1$	646	1.4	$\pi \rightarrow \pi^*$, Eu(4f) $\rightarrow \pi^*$
		$15\ ^8A_1$	640	1.0	$\pi \rightarrow \pi^*$
G	603	$16\ ^8B_1$	614	3.8	Eu(4f) $\rightarrow \pi^*$
		$17\ ^8A_1$	607	5.4	Eu(4f) $\rightarrow \pi^*$
		$17\ ^8B_2$	603	3.8	$\pi \rightarrow \pi^*$
H	509	$23\ ^8B_2$	548	55.7	$\pi \rightarrow \pi^*$
		$25\ ^8A_1$	541	12.7	$\pi \rightarrow \pi^*$

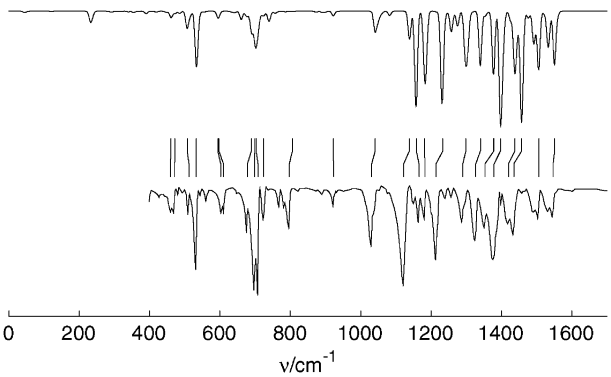

Fig. 3 Experimental (bottom) and calculated (top) infrared spectrum of $Eu@C_{74}$. Experimental data are from ref. 12.

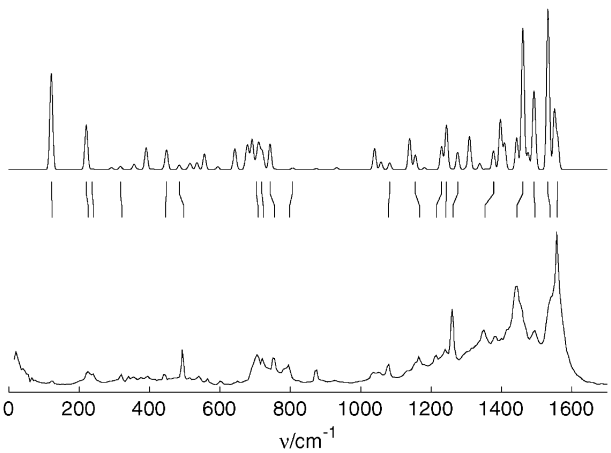

Fig. 4 Experimental (bottom) and calculated (top) Raman spectrum of $Eu@C_{74}$. Experimental data are from ref. 12.

Table 2 Assigned infrared (IR) and Raman spectra of Eu@C_{74}. Vibrational frequencies in cm^{-1} and relative infrared and Raman intensities in % are shown. Experimental data are from ref. 12. Vibrational modes are labeled according to irreducible representations of the C_{2v} point group. Experimental intensities are reported as strong (s), medium (m), weak (w)

Experiment			TDDFT, this work			
Freq./cm^{-1}	IR	Raman	Sym.	Freq./cm^{-1}	IR	Raman
123	—	w	a_1	120.5	0.1	1.6
225	—	m	a_1	219.9	0.0	1.9
240	—	m	a_1	236.9	4.6	0.0
321	—	m	a_1	316.9	0.5	0.3
445	—	m	a_1	441.8	0.0	0.2
			a_1	448.2	1.1	2.5
459	m	—	b_1	461.3	6.1	0.0
471	m	—	b_2	472.0	2.2	0.0
512	m	—	b_2	506.5	16.0	0.0
533	s	—	b_1	532.2	30.3	0.0
			a_1	534.5	24.1	1.1
602	m	—	a_1	593.6	3.8	0.5
610	m	—	b_2	596.7	3.5	0.0
678	m	—	b_1	689.2	12.1	0.0
698	s	—	b_1	699.4	20.6	0.0
708	s	s	a_1	703.0	14.1	1.7
			a_1	707.3	10.7	0.8
			a_1	710.4	5.1	5.2
723/724	m	s	a_1	719.0	2.0	3.8
			a_1	724.3	2.3	1.3
755	—	s	a_1	742.2	2.8	6.3
			a_1	755.9	1.6	0.1
797/798	m	m	a_1	806.4	0.2	0.5
923	m	—	b_1	922.1	4.5	0.0
1031	s	—	a_1	1039.3	2.7	8.0
			b_1	1040.8	16.9	0.0
			b_2	1048.5	9.0	0.0
1079	—	m	a_1	1082.3	4.2	2.6
1122	s	—	b_1	1138.4	17.3	0.0
			a_1	1139.0	10.5	13.1
1166/1167	m	m	a_1	1155.1	11.8	6.3
			b_1	1157.5	82.7	0.0
			b_1	1161.8	2.8	0.0
1183	m	—	a_1	1181.0	42.3	0.8
			b_2	1183.0	6.0	0.1
			b_2	1186.0	37.4	0.0
1214/1215	s	m	a_1	1229.8	44.7	10.8
			b_1	1232.7	52.7	0.0
1242	—	m	a_1	1243.8	0.2	21.0
1262	—	s	a_1	1275.5	14.4	8.5
1290	m	—	b_2	1295.0	11.5	0.1
			a_1	1298.5	34.6	0.6
			b_1	1300.4	3.1	0.0
			b_2	1304.7	27.5	0.0
1327	m	—	a_1	1338.2	9.1	3.2
			b_1	1340.1	45.2	0.0
1350/1353	m	m	a_1	1375.5	9.7	2.1
			a_1	1377.7	38.5	8.3
			b_1	1378.0	15.5	0.0
1379	s	—	a_1	1397.0	100.0	27.4
			b_1	1403.2	37.2	0.0
1420	m	—	b_1	1437.1	18.9	0.0
			b_2	1437.7	34.5	0.0
			a_1	1443.4	21.1	18.3
1435	m	—	b_1	1456.6	66.9	0.0
			a_1	1458.1	31.2	1.0
1444	—	s	a_1	1461.0	16.4	82.2
1495	—	m	a_1	1491.5	28.5	38.4
			a_1	1495.8	6.0	14.5
1506	m	—	b_2	1503.1	8.5	0.0
			b_1	1506.1	50.7	0.0
1538	—	s	a_1	1532.4	29.4	100.0
1547	m	—	a_1	1550.7	47.7	36.8
			b_1	1550.9	4.8	0.0
1558	—	s	a_1	1559.8	0.7	18.2

deviation between calculated and experimental vibrational frequencies is 9 cm^{-1}. Calculated vibrational intensities are more sensitive to methodical errors and environment effects than vibration frequencies, and deviations up to an order of magnitude may occur between theory and experiment. These difficulties notwithstanding, the shapes of the infrared and Raman spectra of Eu@C_{74} are well reproduced. In particular, the division of the vibrational spectra into radial (below *ca.* 800 cm^{-1}) and tangential vibrations (above 1000 cm^{-1}) is clearly distinguishable. The agreement between experimental spectra and theoretical predictions for the considered IPR structure allows us to rule out potential non-IPR isomers of Eu@C_{74} which would lead to significantly different vibrational spectra.[13]

Although Eu@C_{74} does not possess an inversion center and the mutual exclusion rule for vibrational modes does not strictly apply, infrared and Raman spectra of Eu@C_{74} are complementary: all strong Raman bands are polarized, *i.e.*, they correspond to totally symmetric vibrational modes (a_1 in the C_{2v} point group). On the other hand, many intensive infrared absorptions arise from vibrational modes of b_1 or b_2 symmetry, *e.g.*, the bands at 533 cm^{-1} and 698 cm^{-1}. Some totally symmetric vibrations are observed in both infrared and Raman spectrum, *e.g.*, those at 708 cm^{-1} and 1214/1215 cm^{-1}. The radial breathing mode which dominates the Raman spectra of C_{60} and C_{70} appears as a low-intensity band at 445 cm^{-1} in the experiment (442 cm^{-1} in the calculation).[43] The intensive Raman bands above 1400 cm^{-1} are due to tangential bending and stretching motion of the carbon cage. The characteristic pentagonal-pitch mode is found at 1461 cm^{-1}, very close to the frequencies of the corresponding vibrations in C_{60} and C_{70} (1467–1470 cm^{-1}). Two medium-to-strong bands at 497 and 874 cm^{-1} in the experimental Raman spectrum could not be assigned to intensive fundamental vibrational transitions. It is conceivable that these bands correspond to the first overtones of the quadrupolar cage vibration[44] at 240 cm^{-1} (computed value 236 cm^{-1}) and of the cage breathing mode at 445 cm^{-1} (computed value 442 cm^{-1}), respectively. The enhancement of first overtones of these totally symmetric vibrations might be mediated by resonance with electronic excited states close to the experimental excitation frequency.

The most salient vibrational transition in the low-frequency part of the Raman spectrum is the Eu–C_{74} stretching mode which is identified at 123 cm^{-1} in the experimental Raman spectrum. This band is characteristic for endohedral fullerenes and is sensitive to the charge state of the encapsulated metal,[45] see also section 3.4. DFT predicts the vibrational frequency of

the Eu–C_{74} stretching mode at 120 cm^{-1}, in very close agreement with experiment. The calculated Raman scattering cross section of the Eu–C_{74} stretching mode is significantly higher than the experimental one. One possible explanation for this discrepancy is that low-frequency modes involve larger displacements of the cage and are thus more strongly affected by the packing effects present in the experimental spectrum.

3.4 Bonding in Eu@C_{74}

The present DFT results not only provide an assignment of experimental spectra of Eu@C_{74} but also permit an analysis of the metal-cage bonding. The calculated spin expectation value of $S^2 = 15.76$ is very close to the theoretical result of 15.75 for 7 unpaired electrons. Natural population analysis[46] of the occupied molecular orbitals (MOs) suggests that the electronic configuration of europium is best represented as high-spin $4f^7$. Bearing in mind the limitations of population analyses, this finding may be interpreted as europium donating two electrons to the fullerene cage and assuming the oxidation state +2. The high formation energy of the complex from neutral species supports the notion of a predominantly ionic europium–cage bond.

An ionic model for endohedral fullerenes of group 2 and 3 metals has been previously proposed on the basis of theoretical considerations[47] and of empirical linear relationships between the metal-cage stretching frequency and the inverse square root of the atomic mass using a simple electrostatic model.[45] The Eu–C_{74} stretching frequency was found to be in very good agreement with the linear relationship observed for endohedral fullerenes M@C_{74} of alkaline earth metals (M = Ca, Sr, Ba) while it strongly differed from the linear relationship found for the M@C_{82} series (M = Y, La, Ce, Gd) for trivalent cations M^{+3}.[45] This finding was interpreted as additional evidence for europium in the oxidation state +2. Our results support this conclusion and indicate that the electrostatic model is useful for the interpretation of the metal–cage stretching frequencies.

Encapsulation of europium leads to a significant increase of the energy gap between the highest occupied MO (HOMO) and the lowest unoccupied MO (LUMO) from 0.03 eV in the empty C_{74} cage to 0.45 eV in Eu@C_{74}. This reduced reactivity of the fullerene may be a reason why Eu@C_{74} has been synthesized in macroscopic quantities while the isolation of the parent cage C_{74} has been elusive so far.

4. Conclusions

The good agreement of computed and experimental electronic, infrared and Raman spectra indicates that Eu@C_{74} has a C_{2v} symmetric structure derived from the D_{3h} symmetric IPR isomer of C_{74}. This supports the picture of a predominantly ionic fullerene–metal bonding similar to europium sandwich complexes such as Eu(C_5Me_5)$_2$.[40–42] Our results also show that even for large low-symmetric molecules, reasonably accurate interpretation of electronic and vibrational spectra is feasible with modern density functional methods. The presented methodology is widely applicable and represents a viable alternative for systems which are difficult or impossible to study by crystal structure determination, particularly fullerenes. Vibrational spectra have often been regarded as molecular fingerprints, being characteristic but very hard to interpret. The present study demonstrates how computations can help to interpret spectroscopic data and to assign structures, complementing classical structure determination techniques.

Acknowledgements

The authors acknowledge discussions with V. A. Apkarian. The computations for this work were performed at the University of Karlsruhe and were supported by the Center for Functional Nanostructures (CFN) of the Deutsche Forschungsgemeinschaft (DFG) within project C3.9. We acknowledge support by the NSF Center on Chemistry at the Space–Time Limit at UCI (CHE-0533162).

References

1 H. Shinohara, *Rep. Prog. Phys.*, 2000, **63**, 843.
2 S. Guha and K. Nakamoto, *Coord. Chem. Rev.*, 2005, **249**, 1111.
3 J. R. Heflin, D. Marciu, C. Figura, S. Wang, P. Burbank, S. Stevenson and H. C. Dorn, *Appl. Phys. Lett.*, 1998, **72**, 2788.
4 M. Mikawa, H. Kato, M. Okumura, M. Narazaki, Y. Kanazawa, N. Miwa and H. Shinohara, *Bioconjugate Chem.*, 2001, **12**, 510.
5 B. Sitharaman and L. J. Wilson, *J. Biomed. Nanotechnol.*, 2007, **3**, 342.
6 W. Harneit, *Phys. Rev. A: At., Mol., Opt. Phys.*, 2002, **65**, 032322.
7 H. Sinohara, in *Fullerenes: Chemistry, Physics and Technology*, ed. K. M. Kadish and R. S. Ruoff, Wiley, New York, 2000, ch. 8, p. 358.
8 A. L. Balch, in *Fullerenes: Chemistry, Physics and Technology*, ed. K. M. Kadish and R. S. Ruoff, Wiley, New York, 2000, ch. 4, p. 177.
9 T. Zuo, C. M. Beavers, J. C. Duchamp, A. Campbell, H. C. Dorn, M. M. Olmstead and A. Balch, *J. Am. Chem. Soc.*, 2007, **129**, 2035.
10 A. Reich, M. Panthöfer, H. Modrow, U. Wedig and M. Jansen, *J. Am. Chem. Soc.*, 2004, **126**, 14428.
11 H. Nikawa, T. Kikuchi, T. Wakahara, T. Nakahodo, T. Tsuchiya, G. M. A. Rahman, T. Akasaka, Y. Maeda, K. Yoza, E. Horn, K. Yamamoto, N. Mizorogi and S. Nagase, *J. Am. Chem. Soc.*, 2005, **127**, 9684.
12 P. Kuran, M. Krause, A. Bartl and L. Dunsch, *Chem. Phys. Lett.*, 1998, **292**, 580.
13 K. Vietze, G. Seifert and P. W. Fowler, *AIP Conf. Proc.*, 2000, **544**, 131.
14 T. Kodama, R. Fujii, Y. Miyake, S. Suzuki, H. Nishikawa, I. Ikemoto, K. Kikuchi and Y. Achiba, *Chem. Phys. Lett.*, 2004, **399**, 94.
15 J. Xu, T. Tsuchiya, C. Hao, Z. Shi, T. Wakahara, W. Mi, Z. Gu and T. Akasaka, *Chem. Phys. Lett.*, 2006, **419**, 44.
16 P. Deglmann, F. Furche and R. Ahlrichs, *Chem. Phys. Lett.*, 2002, **362**, 511.
17 P. Deglmann, K. May, F. Furche and R. Ahlrichs, *Chem. Phys. Lett.*, 2004, **384**, 103.
18 D. Rappoport and F. Furche, *J. Chem. Phys.*, 2007, **126**, 201104.
19 G. Placzek, in *Handbuch der Radiologie*, ed. E. Marx, Akademische Verlagsgesellschaft, Leipzig, 2nd edn, 1934, vol. VI/2, pp. 209–374.
20 M. M. Sushchinskii, *Raman Spectra of Molecules and Crystals*, Israel Program for Scientific Translations, New York, 1972.
21 J. Neugebauer, M. Reiher, C. Kind and B. A. Hess, *J. Comput. Chem.*, 2002, **23**, 895–910.
22 M. J. Frisch, Y. Yamaguchi, J. F. Gaw, H. F. Schaefer III and J. S. Binkley, *J. Chem. Phys.*, 1986, **84**, 531–532.
23 S. H. Gallagher, R. S. Armstrong, R. D. Bolskar and P. A. Lay and C. A. Reed, J. Am. Chem. Soc., 1997, **119**, 4263–4271.
24 S. H. Gallagher, R. S. Armstrong, W. A. Clucas, P. A. Lay and C. A. Reed, *J. Phys. Chem. A*, 1997, **101**, 2960–2968.
25 A. D. Becke, *Phys. Rev. A: At., Mol., Opt. Phys.*, 1988, **38**, 3098.
26 J. P. Perdew, *Phys. Rev. B: Condens. Matter Mater. Phys.*, 1986, **33**, 8822.

27 K. Eichkorn, O. Treutler, H. Öhm, M. Häser and R. Ahlrichs, *Chem. Phys. Lett*., 1995, **242**, 652.
28 A. Schäfer, H. Horn and R. Ahlrichs, *J. Chem. Phys*., 1992, **97**, 2571.
29 F. Weigend and R. Ahlrichs, personal communication.
30 M. Dolg, H. Stoll and H. Preuss, *J. Chem. Phys*., 1989, **90**, 1730.
31 R. Bauernschmitt and R. Ahlrichs, *Chem. Phys. Lett*., 1996, **256**, 454.
32 F. Furche and D. Rappoport, in *Computational Photochemistry*, ed. M. Olivucci, Elsevier, Amsterdam, 2005, ch. III, vol. 16, p. 93.
33 R. Bauernschmitt, M. Häser, O. Treutler and R. Ahlrichs, *Chem. Phys. Lett*., 1997, **264**, 573.
34 J. P. Perdew, M. Ernzerhof and K. Burke, *J. Chem. Phys*., 1996, **105**, 9982.
35 F. Furche and R. Ahlrichs, *J. Chem. Phys*., 2001, **114**, 10362.
36 J. P. Merrick, D. Moran and L. Radom, *J. Phys. Chem. A*, 2007, **111**, 11683.
37 R. Ahlrichs, M. Bär, M. Häser, H. Horn and C. Kölmel, *Chem. Phys. Lett*., 1989, **162**, 165, current version see http://www.turbomole.com.
38 Z. Slanina, F. Uhlík, X. Zhao, L. Adamowicz and S. Nagase, *Fullerenes, Nanotubes, Carbon Nanostruct*., 2007, **15**, 195.
39 Z. Slanina, K. Kobayashi and S. Nagase, *Chem. Phys*., 2004, **301**, 153.
40 W. J. Evans, *Polyhedron*, 1987, **6**, 803.
41 W. Schumann and H. Genthe, in *Handbook of Physics and Chemistry of Rare Earths*, ed. K. A. Gschneidner, Jr and L. Eyring, North Holland, Amsterdam, 1984, vol. 7, ch. 53, pp. 445–571.
42 M. Kaupp, P. v. R. Schleyer, M. Dolg and H. Stoll, *J. Am. Chem. Soc*., 1992, **114**, 8202.
43 H.-J. Eisler, S. Gilb, F. H. Hennrich and M. M. Kappes, *J. Phys. Chem. A*, 2000, **104**, 1762–1768.
44 H.-J. Eisler, F. H. Hennrich, S. Gilb and M. M. Kappes, *J. Phys. Chem. A*, 2000, **104**, 1769–1773.
45 O. Haufe, M. Hecht, A. Grupp, M. Mehring and M. Jansen, *Z. Anorg. Allg. Chem*., 2005, **631**, 126.
46 A. E. Reed, R. B. Weinstock and F. Weinhold, *J. Chem. Phys*., 1985, **83**, 735–746.
47 S. Nagase, K. Kobayshi, T. Akasaka and T. Wakahara, in *Fullerenes: Chemistry, Physics and Technology*, ed. K. M. Kadish and R. S. Ruoff, Wiley, New York, 2000, ch. 9, p. 395.

